Simplified methodologies for out-of-plane resistance verification of framed-masonry walls

Conference Paper · April 2018

4 authors:


Davorin Penava
Josip Jurar Strossmayer University of Osijek


Filip Anić
Josip Juraj Stossmayer University of Osijek


Lars Abrahamczyk
Bauhaus Universität Weimar


Vasilis Sarhosis
University of Leeds

Simplified methodologies for out-of-plane resistance verification of framed-masonry walls

Filip Anić[1], Davorin Penava[1], Lars Abrahamczyk[2], Vasilis Sarhosis[3]

[1]Josip Juraj Strossmayer University of Osijek, Faculty of Civil Engineering Osijek
[2]Bauhaus-University Weimar, Earthquake Damage Analysis Centre EDAC
[3]Newcastle University, School of Engineering
e-mail: {filip.anic, davorin.penava}@gfos.hr, lars.abrahamczyk@uni-weimar.de, vasilis.sarhosis@newcastle.ac.uk

Abstract

In design for earthquake resistance of reinforced concrete frame structures, unreinforced masonry (URM) infill walls, panels or partitions are considered as non-structural elements. However, if effective structural contact with the frame is such that the infill and frame will have equal deformations (framed-masonry), masonry infill walls should be considered as integrated in the structure and a part of the seismic earthquake system (structural element). The effects of infill walls, with or without openings, on the overall seismic response of structural frames are manifested through increase in stiffness, strength and energy dissipation capacity and the alteration of earthquake resistance distribution throughout the structure. The field of research is divided into three general fields: in-plane response, out-of-plane response and their combinations. This work presents the state of the art of simplified modelling approaches for out-of-plane resistance verification. A parametric study was conducted to address the sensitivity of simplified mathematical models on the structural characteristics of masonry infill walls.

Key words: simplified methodologies, URM infill walls, out-of-plane resistance, framed-masonry walls, sensitivity study

1 Introduction

The interaction between RC or structural steel frames with masonry infill walls is largely unsolved. With insufficient knowledge at the time, many provisions such as European seismic code EN 1998-1 [1] regard infill as a secondary element in seismic excitation. The research on the interaction began in the early 60's with the work by [2, 3]. Since then the field of research has broadened. Worldwide studies were done with the goal of systematic inclusion of infill walls into frame structures.

The characteristical behavior of infill walls and especially its interaction with the frame structure under seismic action can be distinguished into three basic parts: 1. In-plane (IP) interaction; 2. Out-of-plane (OoP) interaction and 3. Out-of-plane interaction with previous in-plane damage (IP+OoP).

In comparison with OoP, IP field can be considered as well researched [4, 5]. This paper investigates analytical OoP approaches applied to a frame specimen from [6] (Fig.3). The majority of OoP experimental studies were conducted with airbags pressuring infill directly, while the frame is supported. This method can be considered suitable for blast design as shown in [7–9]. Fewer research is done by dynamical, shaking table methods. Accordingly, the field of OoP research can be found in the domain of earthquake and blast engineering.

It has been shown that boundary conditions, meaning connection between infill and frame govern failure modes (Fig.1) and load capacity's [10, 11]. There are essentially three arching failure modes: 1) two-way action, when the infill is fully connected to the frame. Failure pattern forms letter X (Fig.1a); 2) One way action, usually the infill and the beam are disconnected, failure pattern forms upside down letter Y (Fig.1b); c) Two opposite sides of infill-frame are disconnected, e.g. both columns or both beams, failure pattern forms perpendicular line between disconnected lines (Fig. 1c).

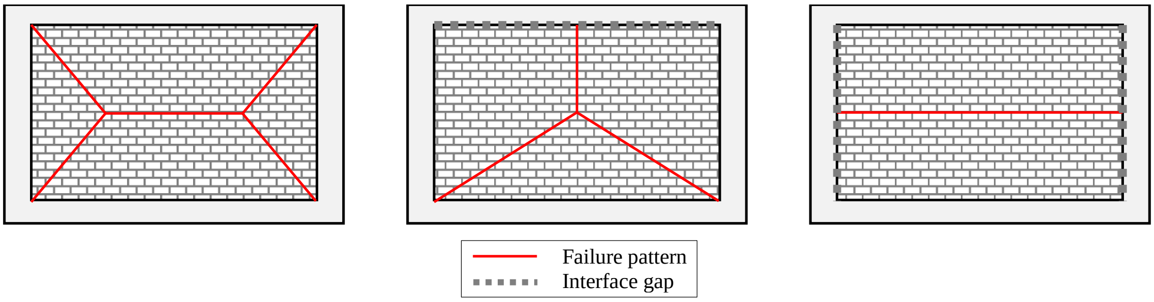

a) Two-way action b) Single gap one-way action c) Double gap one-way action

Figure 1: Failure modes depending on boundary conditions

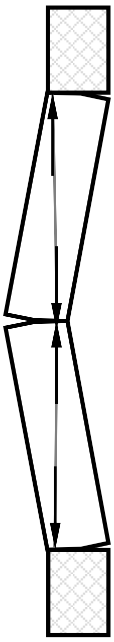

Figure 2: Arching action

The arching action is a failure mode that occurs when first cracks develop, infill divides into *n* parts (depending on boundary conditions) and start to rotate as rigid bodies (fig.3). When the rotation occurs, infill segments clamp and crush on three major points that develop so called "Compression arch". Compression arch provides more capacity to the system and renders its behavior mainly on compressive and geometrical characteristics of the infill wall as it can be observed in Table 3.

The first arching action analytical model was proposed by McDowell [2] in 56's. Many authors followed the same principals. The further development of analytical models included: a) differentiating failure modes by slenderness as a crushing at boundary or transverse instability failure by [12]; b) previous IP damage [13–16]; c) differing two-way from one-way actions [10, 17, 18]; d) calculation of ultimate displacement [13, 17]; e) inclusion of openings [13].

It is to be noted that besides arching action models there are flexural based models [19, 20]. However, those models are depended upon flexural – tensile properties of infill walls. This was shown as unfit when compression arch develops.

Table 1 displays arching action based analytical models with their experimental setup and specific conditions taken into consideration. Table 2 displays ultimate displacement equations. Table 3 displays calculation of ultimate OoP loading. The values and description of symbols can be seen on table 4.

2 Frame & infill wall properties

The specimen used for model comparison (Fig. 3) is obtained from [6] and is consisted of a medium ductility (DCM) RC frame with unreinforced masonry (URM) infill wall. The URM infill wall is consisted of hollow clay blocks categorized as group 2 by EN 1996-1 [21] provisions. Blocks are connected by general purpose mortar designated as M5 by EN 1996-1 [21]. The mechanical properties, obtained experimentally can be found in Table 4.

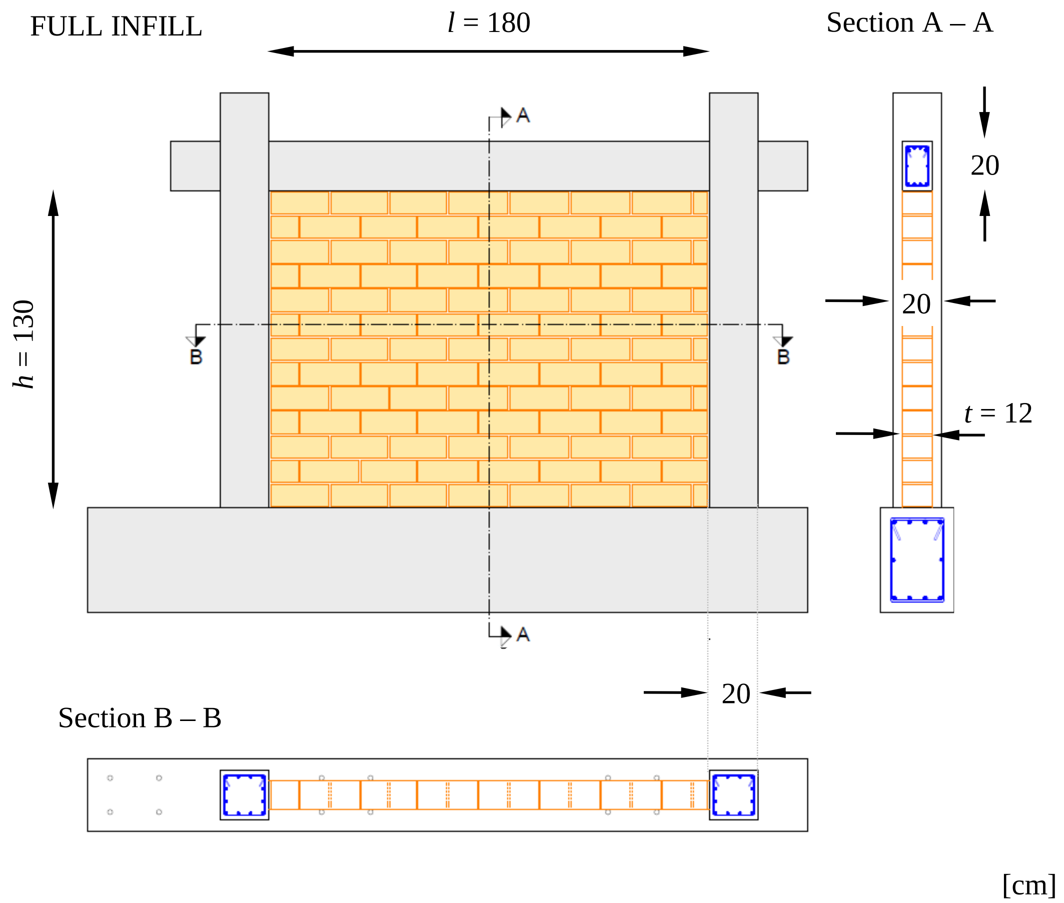

Figure 3: Specimen considered in the study according to [6]

Table 1: Proposed arching action analytical models test setups

#	Author	Test type upon which calculations are based	Frame type	URM type	Specific conditions considered?	OoP ±IP⸸
1	Angel [14]	Cyclic-quasi static with airbag	RC	Double leaf clay brick & hollow conc. blocks	Slenderness	+
2	Dawe [10]	Monotonic with airbag	Steel	Clay brick	Boundary conditions	-
3	Flanagan [22]	Cyclic-quasi static with airbag	Steel	Hollow clay block	Max. displacement, openings considered	+
4	Moghaddam [12]	Dynamic explicit method obtained from [23]	RC*	Hollow clay bricks	Slenderness	-
5	Klingner [17]	Dynamic – shaking table	RC	Clay brick	Max. displacement	+

** It is to be noted that frame was installed just to produce boundary condition*
⸸ OoP ± IP is referred was is tested experimentally

Table 2: Ultimate displacement

#	Author	Ultimate displacement		Action
3	Flanagan [22]	$d = \dfrac{0.002\, h^2/t}{1 + \sqrt{1 - 0.002(h/t)^2}}$	(1)	Two-way
5	Klingner [17]	$x_y = \dfrac{t f_m l}{1000E\left(1 - \dfrac{h}{2\sqrt{(h/2)^2 + t^2}}\right)}$	(2)	Two-way

Table 3: Ultimate OoP load calculation layout

#	Author	Ultimate load		Action	Add	OoP ±IPǂ	Units
1	Angel [14]	$w = R_1 R_2 \dfrac{2 f_m \lambda}{h/t}$	(3)	Two-way	h/t | λ | R_1 | R_2 5 | 0.129 | 0.997 | 0.994 10 | 0.060 | 0.946 | 0.894 15 | 0.034 | 0.888 | 0.789 20 | 0.021 | 0.829 | 0.688 25 | 0.013 | 0.776 | 0.602 30 | 0.008 | 0.735 | 0.540 35 | 0.005 | 0.716 | 0.512	+	US
2	Dawe [10]	$w_3 = \dfrac{800\, f_m^{0.75}\, t^2 (\alpha \le 75)}{l^{2.5}}$	(4)	One-way	$\alpha = \dfrac{1}{h}\left(EI_c h^2 + GJ_c th\right)^{0.25} \le 50$	-	SI
		$w_4 = 800\, f_m^{0.75} t^2 \alpha \left(\dfrac{\alpha}{l^{2.5}} + \dfrac{\beta}{h^{2.5}}\right)$	(5)	Two-way	$\beta = \dfrac{1}{l}\left(EI_b l^2 + GJ_b tl\right)^{0.25} \le 50$		
3	Flanagan [22]	$w = 4.1\, f_m^{0.75} \alpha \left(\dfrac{\alpha}{l^{2.5}} + \dfrac{\beta}{h^{2.5}}\right)$	(6)	Two-way	$\alpha = \dfrac{1}{h}\left(EI_c h^2\right)^{0.25} \le 50$ $\beta = \dfrac{1}{l}\left(EI_b l^2\right)^{0.25} \le 50$ $h/t \le 1/8 \Rightarrow h/t = h/8$	-	SI
4	Moghaddam [12]	$w = \min \begin{cases} w_{cr} = \dfrac{0.85 f_m}{\lambda^2} - \left(0.12 + \dfrac{0.45}{\alpha}\right) \dfrac{f_m^2}{E_m} \\ w_{max} = \dfrac{0.18 E_m}{(0.12 + 0.045/\alpha)\lambda^4} \end{cases}$	(7)	w_{cr} crushing failure Two-way w_{max} transverse instability failure	$\alpha = \dfrac{384 EI_b h}{E_m t l^4}$ $\lambda = h/t$	-	SI
5	Klingner [17]	$w = 8 \dfrac{M_{yv}}{h}(l-h) + 8 M_{yv} \ln(2) + 8 \dfrac{M_{yh}}{h} \dfrac{x_{yv}}{x_{yh}} \ln\left(\dfrac{l}{l - h/2}\right) l$	(8)	Two-way	$x_{yv} = \dfrac{t f_m}{1000 E \left(1 - \dfrac{h}{2\sqrt{(h/2)^2 + t^2}}\right)}$ $M_{yv} = (0.85 f_m / 4)(t - x_{yv})^2$	-	SI

ǂ *OoP ± IP is referred to implementation in calculations ; For calculation of* x_{yv} *replace h with l, and for calculation of* M_{yh} *replace* x_{yv} *with* x_{yh}

Table 4: Material properties from the study of [6]

Properties	Symbol	Value	Unit
Infill wall compressive strength	f_m	17.50	MPa
Young modulus of infill wall	E_m	5650.00	MPa
Young modulus of frame	E	41000.00	MPa
Shear modulus of frame	G	17083.33	MPa
Infills height	h	130.00	cm
Infills thickness	t	12.00	cm
Infills length	l	180.00	cm
Frame column moment of inertia	I_c	1.33×10^{-4}	cm^4
Frame beam moment of inertia	I_b	8.00×10^{-5}	cm^4

3 Results

The results of the applied formulas on the selected specimen frame are presented in Table 5 and Figure 5. In Table 5, the differences in force Δw are compared, whereas the undamaged state according to Angel [13] is taken as an reference. In Figure 5a, the influence of slenderness h/t in range from 5 to 35 was obtained from Angel [13]. For h / t calculations, thickness was set as constant t = 120 mm and height was varied as $h = h/t \cdot t$. Klingner curve in Figure 5 shows results in domain of $h/t < 30$ as for aspect ratio of h/l between 0 and 5 in natural logarithm $\ln(l / (l - h/2))$ Eq.(8) produces complex numbers $\mathbb{C}$ due to $\ln(\mathbb{R}^{-})$. In Figure 5b compression strength of masonry unit f_m was varied. For the variation, a modification of Young modulus E_m was incorporated trough equation 9 & 10 from [21].

$$f_k = K f_m^{0.7} f_{mortar}^{0.3} \tag{9}$$

$$E_m = 1000 f_k \tag{10}$$

Where: $f_b = \delta f_m$; $\delta = 0.783$; $K = 0.45$, $f_{mortar} = 5$ MPa

In Figure 5b the "Actual f_m" line corresponds to E_m= 4556.84 MPa instead of measured E_m= 5650.00 MPa (Tab.4) as a result of Eq.10.

In Figure 5b Moghaddam's w_{max} curve has a slight inclination from 0.3773 to 0.3775 (nearly horizontal line) due to w_{max} in Equation 7 not including the variated parameter f_m. The slight inclination is due to change in E_m.

4 Discussion of results and concluding remarks

With results shown in Table 5 and Figure 5, it can be concluded that:

a) Highly disperse results are obtained. Lowest difference of 6% (Angel – Dawe, two-way) and highest difference of 331% (Angel – Moghaddam) was found.
b) Calculated displacement show immense differences.
c) The results of the slenderness sensitivity analysis (Fig.5a) indicates: higher slenderness $h / t > 17.5$ produces lower differences between analytical models (with the exception of Klingner model). However, for lower slenderness $h / t < 17.5$ especially for $h / t <$

12.5 values of *w* are widely dispersed among each other. This can be explained by noting that EN 1998-1 [1] provisions limit slenderness to < 15. Within the allowed slenderness, models vary excessively, and at higher they are more similar as the slenderness is key factor in instability cases.

d) It was found that Klingner equation (9) has aspect ratio limit of $h / l < 2$ as a consequence of the natural logarithm in the mentioned equation. It is to be noted that such a ratio is not a usual practice in the framed masonry structural systems.
e) In sensitivity analysis of compression strength f_m (fig.5b) it can be observed that by having lower strength, differences are also lower. The remark is stated with the exception of Klinger's w_{max}. Klinger's w_{max} is failure by instability, hence, it does not incorporate f_m in its equation (Eq.9).
f) By comparing Figure 5a & 5b, overall, slenderness had greater impact on the OoP capacity than the compression strength.
g) Dawe's calculations showed that by having no connection between infill and beam w_3 the loss of capacity in comparison to fully connected infill – frame w_4 resulted in 62% difference.
h) By comparing Dawes one-way w_3 and two-way w_4 action in Figure 5 it is obvious that two-way w_4 action has greater capacity than the one-way w_3 action.
i) Taking into account Moghaddam's division of failure modes by crushing at the boundary w_{cr} and transverse instability w_{max}, the crushing failure curve is significantly lower than the transverse instability curve.
j) Angels previous IP damage showed significant reduction of OoP capacity (up to 13%).

In summation, it can be concluded that analytical models widely differ from each other. This can be attributed to the fact that all analytical models were based on different infill, frame and testing setup.

Table 5: Results of calculations

#	Author	OoP max. load		OoP max. displ.	
		w (MPa)	Δw (%)	d (mm)	Δd (%)
1	Angel undamaged [14]	0.087	0.000		
2	Angel medium damage [14]	0.082	5.957		
3	Angel heavy damage [14]	0.076	12.707		
4	Dawe one-way w_3 [10]	0.031	64.657		
5	Dawe two-way w_4 [10]	0.082	5.592		
6	Klingner [17]	0.130	-48.730	15.024	0.000
7	Flanagan [22]	0.249	-184.881		
8	Moghaddam w_{max} [12]	0.377	-331.841		
9	Moghaddam w_{cr} [12]	0.014	83,75	0.022	99.854

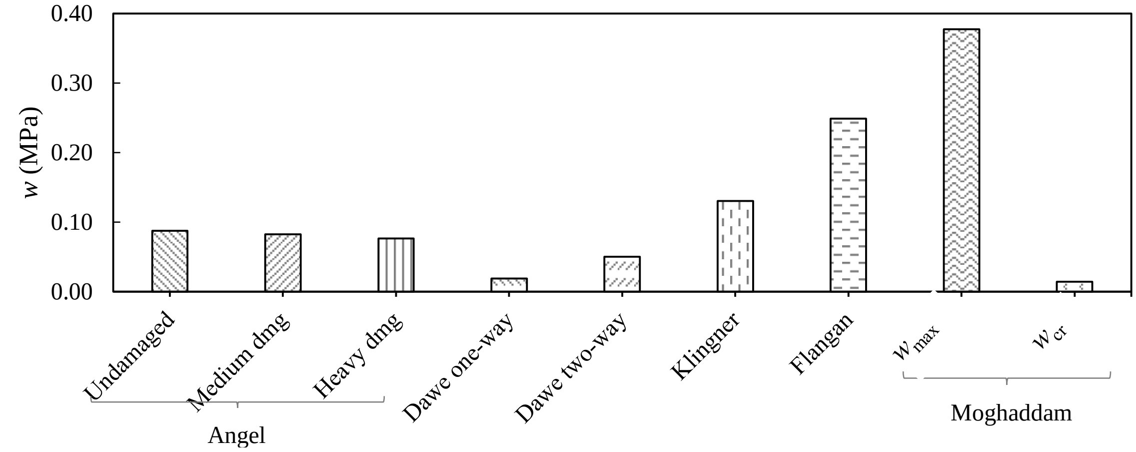

Figure 4: Results of calculations

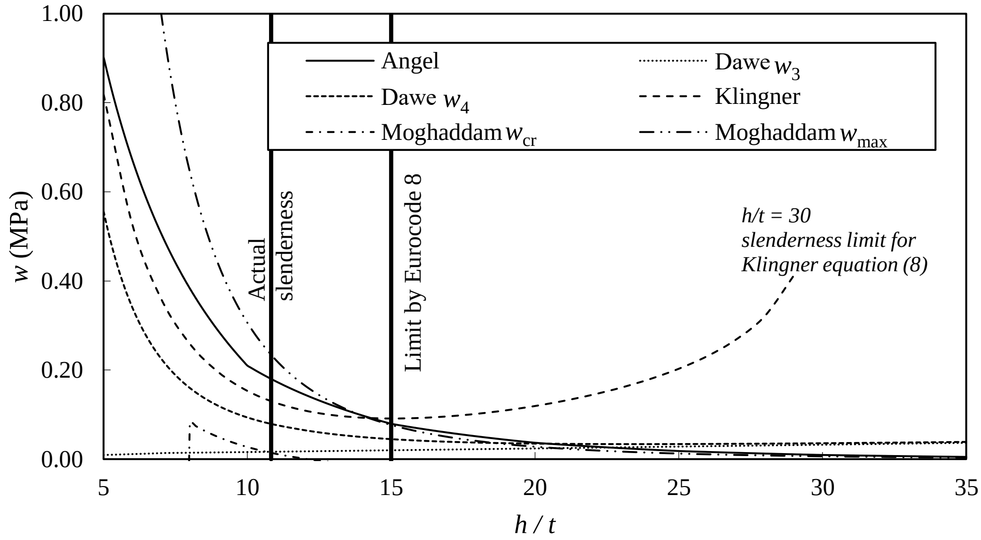

a) Slenderness

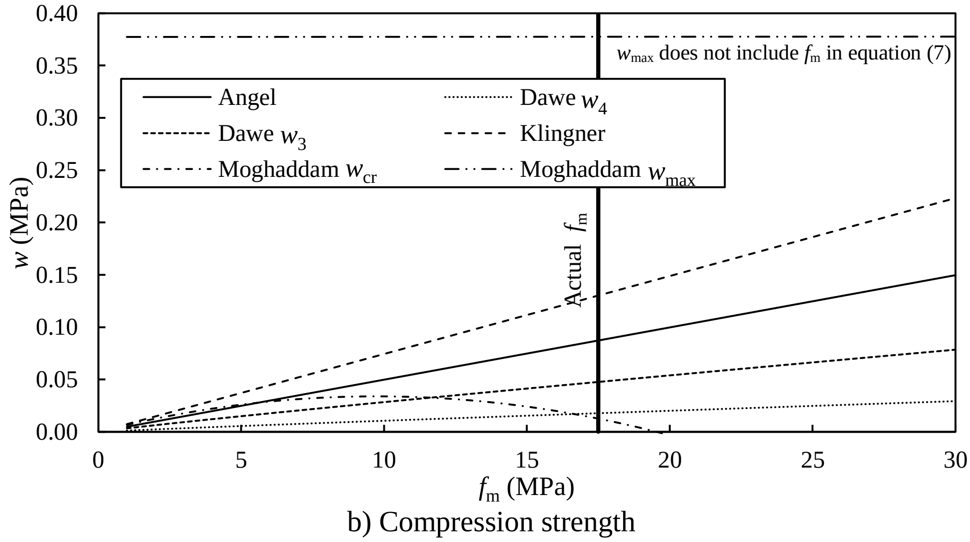

b) Compression strength

Figure 5: Effect of the property variations

References

[1] CEN. Eurocode 8: Design of Structures for Earthquake Resistance - Part 1: General Rules, Seismic Actions and Rules for Buildings (EN 1998-1:2004). Brussels: European Committee for Standardization; 2004.

[2] McDowell EL, McKee KE, Sevin E. Arching Action Theory of Masonry Walls. J Struct Div 1956;82:1–8.

[3] Holmes M. Steel frames with brickwork and concrete infilling. Proc. Inst. Civ. Eng., 1961. doi:10.1680/iicep.1961.11305.

[4] Asteris PG, Antoniou ST, Sophianopoulos DS, Chrysostomou CZ. Mathematical macromodeling of infilled frames: state of the art. J Struct Eng 2011;137:1508–17. doi:10.1061/(ASCE)ST.1943-541X.0000384.

[5] Teni M, Grubišić M, Guljaš I. Simplified Approaches For Modeling Infilled Frames. Elektron Časopis Građevinskog Fak Osijek 2014:70–88. doi:10.13167/2014.9.8.

[6] Sigmund V, Penava D. Influence of openings, with and without confinement, on cyclic response of infilled r-c frames — an experimental study. J Earthq Eng 2014;18:113–46. doi:10.1080/13632469.2013.817362.

[7] Mays GC, Hetherington JG, Rose TA. Response to blast loading of concrete wall panels with openings. J Struct Eng 1999.

[8] Parisi F, Balestrieri C, Asprone D. Out-of-plane blast capacity of load-bearing masonry walls 2016:991–8.

[9] Hrynyk TD, Myers JJ. Out-of-Plane Behavior of URM Arching Walls with Modern Blast Retrofits: Experimental Results and Analytical Model. J Struct Eng 2008;134:1589–97. doi:10.1061/(ASCE)0733-9445(2008)134:10(1589).

[10] Dawe JL, Seah CK. Out-of-plane resistance of concrete masonry infilled panels. Can J Civ Eng 1989;16:854–64. doi:10.1139/l89-128.

[11] Akhoundi F, Vasconcelos G, Lourenco P, Silva L. Out-of-plane response of masonry infilled RC frames : Effect of workmanship and opening. In: Modena C, F. da P, Valluzzi MR, editors. 16th Int. Brick Block Mason. Conf., Padova, Italy: CRC Press/Balkema; 2016, p. 1147–54.

[12] Moghaddam H, Goudarzi N. Transverse resistance of masonry infills. ACI Struct J 2010;107:461–7.

[13] Flanagan RDRDRD, Bennett RMRMRM. Bidirectional behavior of structural clay tile infilled frames. J Struct Eng 1999. doi:10.1061/(ASCE)0733-9445(1999)125:3(236).

[14] Angel R, Abrams DP, Shapiro D, Uzarski J, Webster M. Behavior of reinforced concrete frames with masonry infills. University of Illinois Engineering Experiment Station. College of Engineering. University of Illinois at Urbana-Champaign.; 1994.

[15] Abrams DP, Angel R, Uzarski J. Out-of-Plane Strength of Unreinforced Masonry Infill Panels. Earthq Spectra 1996;12:825–44. doi:10.1193/1.1585912.

[16] Shapiro D, Uzarski J, Webster M, Angel R, Abrams D. Estimating Out-Of-Plane Strength of Cracked Masonry Infills. San Francisco, USA: 1994.

[17] Klinger R, Rubiano, NESTOR R Bashandy, TAREK R Sweeney S. Evaluation and analytical verification of shaking table data from infilled frames. Mason Soc J 1997;15:33–41.

[18] Klingner RE, Rubiano N, Bashandy TR, Sweeney SC. Evaluation of analytical verification of shaking table data from infilled frames. Mason Soc J 1997;15:33–41.

[19] Hendry A. The lateral strength of unreinforced brickwork. Struct Eng 1973:43–50.

[20] Drysdale RG, Essawy AS. Out-of-plane bending of concrete block walls. J Struct Eng 1988. doi:10.1061/(ASCE)0733-9445(1988)114:1(121).

[21] CEN. Eurocode 6: Design of masonry structures - Part 1-1: General rules for reinforced and unreinforced masonry structures (EN 1996-1-1:2005). Brussels: European Committee for Standardization; 2005.

[22] Flanagan RD, Bennett RM. Arching of Masonry Infilled Frames: Comparison of Analytical Methods. Pract Period Struct Des Constr 1999;4:105–10. doi:10.1061/(ASCE)1084-0680(1999)4:3(105).

[23] Galati N, Tumialan JG, Nanni A, Tegola A La. Influence of Arching Mechanism in Masonry Walls Strengthened with FRP Laminates. ICCI 2002, 2002.